

# A Method to Search for $\mu \rightarrow e\gamma$ Decays with High Intensity Muon Sources.

Fritz DeJongh\*

*Fermilab*

January 6, 2005

## Abstract

Muon beamlines such as the one being designed for the MECO experiment will provide a large increase in muon stopping rates, allowing for possible large increases in sensitivity to  $\mu \rightarrow e\gamma$ . As higher-power proton-drivers become available, even higher rates will become possible.

We have analyzed the capabilities of a detector for  $\mu \rightarrow e\gamma$  using pixel detectors to track the positron, and a conversion pair from the photon. We find that an initial detector with a beamline comparable to MECO and 10% of the coverage of the MEGA experiment can already be competitive with experiments currently under construction with a modest amount of live-time. By increasing the coverage and running longer, it should be possible to go further.

We have found that the accidental backgrounds depend strongly on the thickness of the photon converter, providing a way to make continued major progress as improved pixel detectors and more intense muon sources become available.

---

\*fritzd@fnal.gov

# 1 Introduction

The muon was discovered in cosmic rays in 1937 by Neddermeyer and Anderson [1]. Further experiments in cosmic rays showed that the muon is apparently a copy of the electron with 200 times the mass and a lifetime of  $2\ \mu\text{sec}$ , prompting the famous comment by Rabi: “Who ordered that?” It was natural to guess that the muon might decay into an electron and photon, and the first search for this decay mode was performed by Hincks and Pontecorvo [2] in 1948. They concluded that:

Each decay electron is not accompanied by a photon of about 50 MeV.

Their data indicates a branching ratio of less than about 10%. The current best upper limit on the  $\mu^+ \rightarrow e^+\gamma$  branching ratio is from the MEGA collaboration at LANL:  $< 1.2 \times 10^{-11}$  [3].

Searches for  $\mu \rightarrow e\gamma$  are done with muons stopped in thin targets. Standard muon decays, and standard radiative muon decays, produce electrons and photons. The main background to  $\mu^+ \rightarrow e^+\gamma$  arises from accidental coincidences between electrons and photons near the kinematic endpoint of these standard processes. The rate of this background is proportional to the square of the instantaneous muon intensity, thus higher duty cycles are better. The MEG experiment at the PSI aims for sensitivity at the  $10^{-14}$  level [4] by using a 100% duty cycle, compared to 6% for MEGA, and also improving the electron and photon resolution.

Until a  $\mu \rightarrow e\gamma$  signal is observed, new experiments will aim for sensitivity to lower branching ratios. Once a signal is observed, the goal will be to obtain a large number of events for precision measurements. Either goal will require increasing the rate of stopped muons. The difficulty arises from the fact that the effective branching ratio of the accidental backgrounds increases linearly with the rate of stopped muons. Therefore, progress in the stopped muon rate must proceed in tandem with improvements in detector rate capabilities as well as detector resolution.

To accomplish this, future generations of experiments can exploit two general trends in the field of high energy physics:

1. The development of high-power proton drivers. The collision of a proton beam with a target produces pions, which decay to muons. Proton drivers are also used as the front-end of high-energy hadron colliders,

as well as for the production of neutrinos, kaons, neutrons, and antiprotons.

2. The development of thin, high-rate pixel detectors. The interest in tagging  $b$ ,  $c$ , and  $\tau$  particles in high-luminosity colliders is driving the continuous improvement in precision tracking technology. The excellent hit resolution and pattern recognition capabilities of these detectors allow tracking resolution to be improved to near the limits from energy loss and multiple scattering.

Current examples of muon beams can be found at the PSI and AGS proton sources. The PSI cyclotron produces a 1 MW continuous beam of 590 MeV protons [5]. A surface muon beam is produced from stopped pions. The  $\mu \rightarrow e\gamma$  experiment planned for PSI will use up to  $2 \times 10^8$  stopped muons/sec. The continuous beam is well suited to a measurement such as the search for  $\mu \rightarrow e\gamma$ , which requires a coincidence between the two final state particles.

The MECO experiment [6] is being proposed to run at the AGS, with a goal of obtaining a sensitivity of  $10^{-16}$  in the fraction of  $\mu^- \rightarrow e^-$  conversions in the nucleus of Aluminum. The AGS will provide a pulsed source of 8 GeV protons at a power of 0.02 MW. With a pion capture solenoid and a decay channel, it is possible to obtain of order  $10^{11}$  stopped muons/sec [7]. The pulsed structure is very suitable for experiments such as MECO, where the signal is the appearance of a single electron on the time scale of the muon lifetime.

Proton drivers with power of 1 MW or more are currently being designed [8, 9, 10]. Accumulator rings will be necessary to turn the pulsed structure of the proton drivers into a continuous beam. At the Fermilab site, for example, it may be possible to adapt the antiproton recycler for this purpose [10]. At the price of reduced efficiency, it should also be possible to produce highly polarized muons. Given the projected performance of the MECO beamline design, it is apparent that vast increases in stopped muon rates will be possible.

The BTeV collaboration has been developing planes of Silicon pixels for use in a hadron collider environment with a very high track density [11]. These pixels are designed for a flux as high as  $10^{14}$  particles/cm<sup>2</sup>/year, and a hit resolution of about 5  $\mu$ m. One drawback is their thickness: 0.9% of a radiation length.

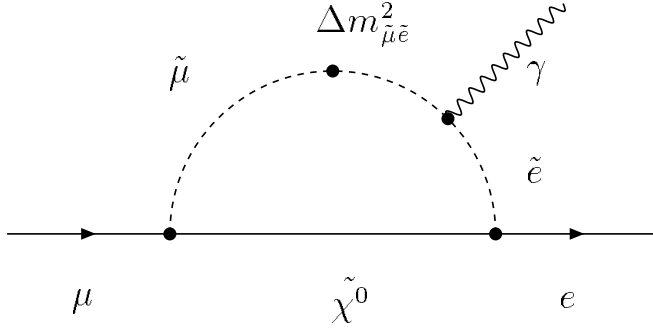


Figure 1: Feynman diagram for  $\mu \rightarrow e\gamma$  induced by slepton flavor mixing.

CCD pixel arrays are being developed for high-energy electron–positron colliders [12]. While these detectors do not have a high flux capability, they are very thin,  $<0.1\%$  of a radiation length, have excellent hit resolution, and so provide precise tracking with very little multiple scattering or energy loss.

Ultimately, monolithic pixel arrays [13] may provide the best of both worlds: high flux ability with a thin detector.

## 2 Theoretical motivation

Currently, the only fundamental particles known to decay through a radiative transition to another particle are the  $s$ - and  $b$ -quarks, with  $BR(b \rightarrow s\gamma) = (2.7 \pm 0.5) \times 10^{-4}$  [14]. This branching ratio is well-explained in the standard model through second-order electroweak processes involving quark mixing.

In the lepton sector, atmospheric muon neutrinos have been observed to oscillate into other flavors of neutrinos, and this essentially constitutes an observation of muon number violation. Neutrino oscillations imply the existence of non-degenerate neutrino masses, and mixing between the mass and flavor eigenstates. In muon decays, the Lepton Flavor Violating (LFV) effects from neutrino masses and mixing are suppressed by the small neutrino masses and are far too small to be observable. However, neutrino oscillations generically imply the existence of LFV operators at high mass scales which can have observable effects in muon decays [15]. For example, Fig. 1 illustrates a possible mechanism for  $\mu \rightarrow e\gamma$  in supersymmetric models. Mechanisms such as this might contribute at levels close to current upper bounds.

When a negative muon is stopped in some material, it will be captured by

an atom, and cascade down to the 1s state. In the standard model, the muon will either decay in orbit, or be captured by the nucleus with the emission of a  $\nu_\mu$ . In models of physics beyond the standard model, the muon can interact with the nucleus and be converted into an electron. The signature for such an event is the production of an electron with an energy beyond the kinematic endpoint of the decay in orbit. Since non-photonic diagrams can contribute to  $\mu^- \rightarrow e^-$  conversion, this measurement is complementary to  $\mu^+ \rightarrow e^+ \gamma$ .

Once the decay  $\mu \rightarrow e \gamma$  has been observed, it will become important to conduct the observation with polarized muons, in order to obtain information on the handedness of the interaction responsible for the decay.

### 3 Accidental backgrounds

Accidental backgrounds arise from the coincidence of two muon decays in the target: One producing a positron from a  $\mu \rightarrow e \nu \bar{\nu}$  decay, the other producing a photon from a  $\mu \rightarrow e \nu \bar{\nu} \gamma$  decay. External bremsstrahlung and annihilation in flight of the  $e^+$  also contribute to photon backgrounds. While the signal rate for  $\mu \rightarrow e \gamma$  decays is proportional to  $R_\mu$ , the stopping rate of muons in the target, the accidental background is proportional to  $R_\mu^2$ . Thus, we have the dilemma in trying to improve sensitivity to  $\mu \rightarrow e \gamma$ : Increasing  $R_\mu$  to obtain more signal also reduces the purity of the signal, and can end up degrading the sensitivity.

The sensitivity of a  $\mu \rightarrow e \gamma$  search is therefore limited by  $B_{acc}$ , the effective branching ratio of the accidental background. An estimate of this parameter can be obtained with the following formula [16]:

$$B_{acc} = \left( \frac{R_\mu}{d} \delta t_{e\gamma} \right) \cdot (\delta x) \cdot \left( \frac{\delta y}{15} \right)^2 \cdot \left( \frac{\delta \theta_{e\gamma}^2}{4} \right) \cdot \left( \frac{(2\delta \theta_z L_{\gamma T})^2}{A_T} \right) \quad (1)$$

where  $\delta x$  is the positron relative energy resolution,  $\delta y$  is the photon relative energy resolution,  $\delta \theta_{e\gamma}$  is the resolution on the angle between the electron and photon, and  $\delta t_{e\gamma}$  is the resolution on the relative timing of the photon and positron. All these resolutions are specified at FWHM.

An experiment such as MEGA measures the photon by reconstructing a conversion pair. In this case, the photon reconstruction provides an additional measurement of the photon direction, called the photon traceback angle, which can be used to extrapolate the photon back to the target and

test for consistency with the muon decay point. In this case,  $\delta\theta_z$  is the resolution for the photon traceback angle,  $L_{\gamma T}$  is the distance from the muon decay point to the photon conversion point, and  $A_T$  is the area of the target. We have assumed that the electron extrapolation is much more precise than for the photon, and the traceback angle resolution is the same in both dimensions.

## 4 Physics background

The decay  $\mu \rightarrow e\nu\bar{\nu}\gamma$  has a branching ratio of about 1.4% for  $E_\gamma > 10$  MeV [14]. In the rare cases that the neutrinos are near rest in the muon rest frame, this decay mimics the  $\mu \rightarrow e\gamma$  signal. The fraction of these events that fall in the signal region depends on the precision of the  $e$  and  $\gamma$  reconstruction [15]. The effective branching ratio of this background is about  $10^{-15}$  for  $e$  and  $\gamma$  resolutions of about 1%. This background decreases as the sixth power of various combinations of kinematical resolutions, so large reductions in this background may become practical.

## 5 Detector Resolution

In this section we discuss the factors that determine the detector resolution, and simple prescriptions to estimate the resolution.

### 5.1 Positron Energy Resolution

The positron energy is measured from its curvature in a magnetic field. Assuming the tracking detectors have adequate position resolution, the energy resolution is determined by fluctuations in energy loss and multiple scattering as the positron exits the target and traverses the detector material.

Fig. 2 shows a detector configuration for which two sets of Silicon trackers measure the position and direction of the track,  $180^\circ$  apart on the trajectory. The position resolution of Silicon detectors is excellent, and shouldn't be a limitation in the energy resolution. The direction measurements will be limited by multiple scattering in the Silicon. However, as shown in Fig. 3, multiple scattering contributes at only 2nd order to the energy resolution for this configuration. Therefore, the energy resolution will be determined by the fluctuations in energy loss in the target and first set of Silicon trackers.

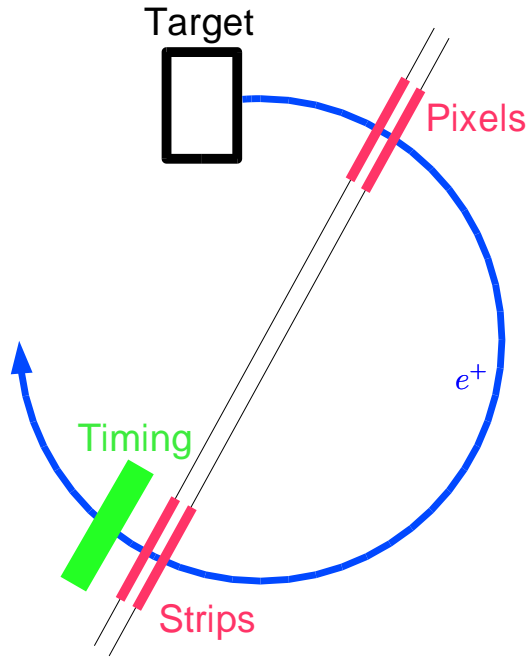


Figure 2: positron tracker

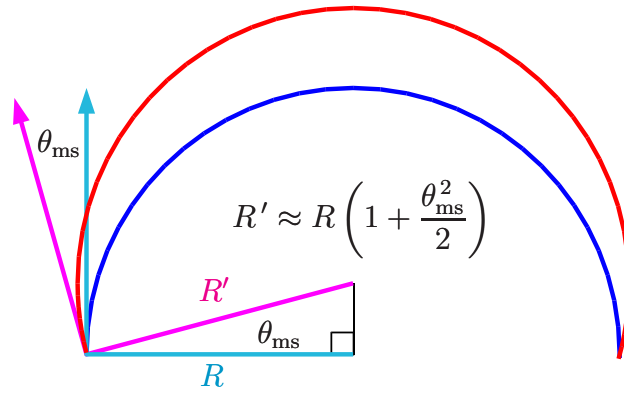


Figure 3: The position of the track in Fig. 2 is very well measured, but multiple scattering causes some uncertainty in the direction. This diagram illustrates how this uncertainty contributes at 2nd order to the curvature resolution.

The PDG Review [14] contains information on fluctuations in energy loss in Silicon detectors. The FWHM of the distribution is about 33% of the most probable energy loss.

## 5.2 Photon Energy and Pointing Resolution

We will concentrate on detectors, such as MEGA, that reconstruct photons via the reconstruction of a conversion pair. The design of such a detector entails a tradeoff between efficiency and resolution. The more material, the higher the conversion efficiency, while energy loss and multiple scattering of the conversion pair in the material limits the energy resolution. For example, the MEGA pair spectrometer uses two lead foils per conversion layer, with 5% of a radiation length each. The energy resolutions are 3.3% and 5.7% (FWHM) in the outer and inner foils respectively.

We assume that, as for the positron tracker, a design with Silicon tracking can be found for which the energy loss will be the dominant contribution to the resolution. In this case, the resolution will be proportional to the converter thickness. Detailed simulations will be needed to explore this issue.

The reconstruction of the conversion pair provides a reconstruction of the direction of the photon, called the photon traceback angle. The pointing resolution will be dominated by multiple scattering in the converter material. The resolutions for the MEGA detector are 67 and 116 mrad for the outer and inner foils respectively. These resolutions can be accounted for almost exactly with a simple estimate of the average multiple scattering of the conversion pair in the converter, with the assumption that each member of the pair provides an independent measure of the photon direction. This resolution will scale as the square root of the amount of conversion material.

## 5.3 Resolution on the positron–photon opening angle

In the detection of a  $\mu \rightarrow e\gamma$  candidate, the location of the muon decay is found by extrapolating the positron trajectory to the muon stopping target. The photon direction is then the vector from the muon decay point to the photon interaction point. If the position of the positron and photon conversion are well measured, the resolution on this opening angle will be limited by the reconstruction of the positron direction. For the configuration in Fig. 2 this will be limited by the multiple scattering in the target and first positron



tracking detector. This resolution will then scale as the square root of the thickness of the stopping target and first tracking layer.

## 5.4 Timing resolution

It is of course essential to have a precise timing measurement for both the positron and at least one member of the conversion pair.

# 6 Dependence of accidental backgrounds on the converter thickness

The photon detector consists of converter foils and tracking layers. For the following discussion, we will assume a fixed number of tracking layers, and examine the level of accidental background as a function of the converter thickness,  $t_c$ . As  $t_c$  decreases, the photon energy and pointing resolution improves, but the conversion efficiency decreases. One way to compensate for this is to increase  $R_\mu$ :

$$N_{e\gamma} \propto R_\mu t_c. \quad (2)$$

For a fixed  $N_{e\gamma}$  we then have:

$$R_\mu \propto t_c^{-1}. \quad (3)$$

From the discussion in Section 5.2 we have:

$$\delta y \propto t_c, \quad (4)$$

$$\delta\theta_z \propto \sqrt{t_c}. \quad (5)$$

Combining equations (4), and (5) with equation (1) we find, for fixed  $R_\mu$ :

$$B_{acc} \propto t_c^3. \quad (6)$$

Applying equation (3) we find, for fixed  $N_{e\gamma}$ :

$$B_{acc} \propto t_c^2. \quad (7)$$

We find that if the detector can handle the rate, there is a strong preference for increasing the muon stopping rate as much as possible and decreasing the converter thickness.

## 7 Extrapolation from the MEGA geometry

In this section, we describe a design for a first generation detector, by adopting the Mega design but with pixel tracking detectors. We assume a muon beam similar to that designed for MECO. We then extrapolate the expected performance based on the achieved MEGA performance.

### 7.1 Target

The MECO experiment is aiming for  $\approx 10^{11}$  stopped muons/sec with 17 Aluminum targets perpendicular to the beam. The MEGA experiment had a single Mylar target for which the normal to the target plane was inclined at  $83^\circ$  with respect to the muon beam. The projected length of the beam through the target is then 8 times the thickness of the target.

We assume a MEGA-style target with a MECO-style beamline, tuned to achieve a muon stopping rate of  $1.5 \times 10^{10}$ /sec, which is easily achievable given the MECO performance.

### 7.2 Positron tracker

For the positron tracker, a possible configuration is shown in Fig. 2. The target will be surrounded by pairs of inner detectors, with fans of outer detectors and timing counters arrayed around the outside of the tracking barrel. One possibility for a first generation detector is to use the BTeV pixel technology. The energy loss of a relativistic positron through two layers of BTeV pixels is about 0.75 MeV, leading to an energy resolution of order 0.5% FWHM, compared to the MEGA performance of 1% FWHM. The pulse height measurement in the pixels may allow the recovery of some of this resolution.

The multiple scattering of a 52 MeV positron in one BTeV pixel layer is about 20 mrad (47 mrad FWHM), which determines the resolution on the positron-photon opening angle. The MEGA performance was 33 mrad FWHM.

Given the readout speed of the BTeV pixels and the muon stopping rate we are aiming for, we expect only a few tracks/cm<sup>2</sup> at a time in the inner trackers, and pattern recognition should not be a problem. The two pixel detectors need only be separated by about a millimeter.

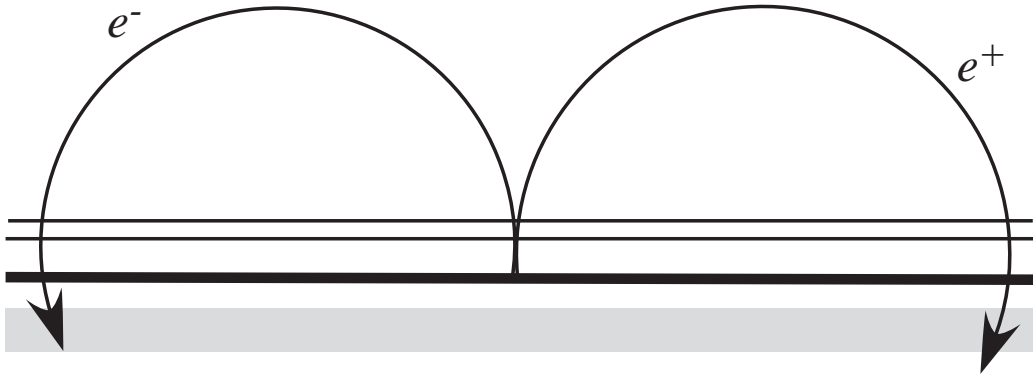


Figure 4: Photon detector. The scintillator bars are on the inside, followed by a depleted Uranium converter, followed by a pair of CCD tracking detectors.

### 7.3 Photon detector

A sketch of a possible photon detector is shown in Fig. 4. This basically follows the MEGA design, with the detector placed outside the maximum radius (30 cm) reached by the positrons from muon decays. While CCD pixel arrays have a much longer readout time than BTeV pixels, (by a factor of about 1000) the absence of positrons and the larger distance from the target should keep their occupancy to a manageable level. As with the positron tracker, the measurement of the trajectory at two points 180° apart should keep the contribution to the energy resolution from multiple scattering low.

As with MEGA, we assume the converter consists of 5%  $X_0$  depleted Uranium. The average energy loss of a conversion pair would be 0.3 MeV, allowing for a photon energy resolution of order 0.2% FWHM. Where MEGA has two converters per tracking layer, we assume only one, so the conversion efficiency will be half that for MEGA. The MEGA performance was 3.2% for conversions originating in the outer of their two converters, and 5.7% for the inner.

The resolution on the photon traceback angle should be the same as for MEGA for photons originating in the outer of their two converters.

### 7.4 Timing detectors

The MEGA achieved timing resolution was 1600 psec FWHM. We assume this can be improved by a factor of 10.

## 7.5 Performance

With a live-time of  $8 \times 10^6$  sec, the MEGA collaboration achieved the following one-event sensitivities, and accidental background level:

$$B_{1-event} \approx 2 \times 10^{-12} \quad (8)$$

$$B_{acc} \approx 2 \times 10^{-12} \quad (9)$$

We assume a detector with the same live-time, same coverage, half the amount of converter material, and 1000 times the muon stopping rate with 100% duty factor. We use Eq. (1) and the assumptions on resolution stated above to scale from the achieved MEGA performance. We find:

$$B_{1-event} \approx 4 \times 10^{-15} \quad (10)$$

$$B_{acc} \approx 1 \times 10^{-14} \quad (11)$$

We note that an initial detector with only 10% of the coverage of MEGA would have performance comparable to the MEG proposal at PSI, even with a modest amount of live-time. As discussed in Section 6

## 8 Further improvements

As higher rate and thinner pixel detectors become available, it will be possible to design experiments with much improved sensitivity. Ultimately, the arrival of monolithic pixel detectors combined with more intense muon beams from the next generation of proton drivers will allow a huge leap forward.

In particular, the use of the relatively thick BTeV pixels for the inner positron tracker is a major limitation. If it were possible to use thinner detectors in just this place, it would have a major benefit on positron energy resolution and photon-positron angle resolution.

Additional detector optimizations should also be possible. For example, the use of a larger  $B$ -field would make the detector more compact and improve the extrapolation of photons to the target.

## 9 Conclusions

MECO-style beamlines will provide a large increase in muon stopping rates, allowing for possible large increases in sensitivity to  $\mu \rightarrow e\gamma$ . However, the

large rates put large demands on the detector while requiring improved resolution to control backgrounds. The position resolution and pattern recognition capabilities of pixel detectors allow for tracking particles to precision near the limits allowed by energy loss and multiple scattering.

We have analyzed the capabilities of a detector for  $\mu \rightarrow e\gamma$  using pixel detectors to track the positron and the conversion pair from the photon. We find that an initial detector with a MECO-style beamline and 10% of the coverage of the MEGA experiment can already be competitive with the MEG proposal with a modest amount of live-time. By increasing the coverage and running longer, it should be possible to go well beyond MEG.

We have found that the accidental backgrounds depend strongly on the thickness of the photon converter. As muon stopping rates are increased, a simple scaling law shows that it is possible to maintain or increase signal rates while steeply reducing accidental backgrounds by decreasing the converter thickness an appropriate amount.

As improved pixel detectors and more intense muon sources become available, it should be possible to make further major improvements. For example, monolithic pixel detectors for the inner positron trackers would allow for a major improvement in the resolution on the positron energy and positron-photon opening angle.

## References

- [1] S. H. Neddermeyer and C. D. Anderson, Phys. Rev. **51**, 884 (1937).
- [2] E. P. Hincks and B. Pontecorvo, Phys. Rev. **73**, 257 (1948).
- [3] M. L. Brooks *et al.* [MEGA Collaboration], Phys. Rev. Lett. **83**, 1521 (1999) [hep-ex/9905013].
- [4] L. M. Barkov *et al.* <http://meg.psi.ch/doc/prop/index.html>
- [5] H.-K. Walter, KEK International Workshop on High Intensity Muon Sources (HIMUS 99), Tsukuba, Japan, 1-4 Dec 1999.
- [6] M. Bachman *et al.* <http://meco.ps.uci.edu/>
- [7] V. L. Tumakov, KEK International Workshop on High Intensity Muon Sources (HIMUS 99), Tsukuba, Japan, 1-4 Dec 1999.

- [8] R. Alber *et al.*,  
<http://www-bd.fnal.gov/pdriver/reports.html>
- [9] Chapter 2 of “Feasibility Study-II of a Muon-Based Neutrino Source”,  
 editors S. Ozaki, R. Palmer, M. Zisman, and J. Gallardo, BNL-52623,  
 June 2001; available at <http://www.cap.bnl.gov/mumu/studyii/FS2-report.html>.
- [10] Bill Foster, “8 GeV Injector Linac Study”,  
<http://tdserver1.fnal.gov/foster/>
- [11] The BTeV proposal,  
[http://www-btev.fnal.gov/public\\_documents/btev\\_proposal/index.html](http://www-btev.fnal.gov/public_documents/btev_proposal/index.html)
- [12] C. Damerell [LCFI collaboration], LC-DET-2001-023 *In \*2nd ECFA/DESY Study 1998-2001\* 1670-1684.*
- [13] G. Deptuch *et al.*, LC-DET-2001-017 *In \*2nd ECFA/DESY Study 1998-2001\* 1574-1583.*
- [14] S. Eidelman *et al.* [Particle Data Group Collaboration], Phys. Lett. B **592**, 1 (2004).
- [15] For a review, see Y. Kuno and Y. Okada, Rev. Mod. Phys. **73**, 151 (2001) [hep-ph/9909265].
- [16] M. Ahmed *et al.* [MEGA Collaboration], Phys. Rev. D **65**, 112002 (2002) [arXiv:hep-ex/0111030].